

Structural evolution in elliptical galaxies: the age – shape relation

Barbara S. Ryden^{1*}, Duncan A. Forbes² and A.I. Terlevich³

¹*Department of Astronomy, The Ohio State University, Columbus OH 43210 USA*

²*Centre for Astrophysics & Supercomputing, Swinburne University, Hawthorn VIC 3122, Australia*

³*School of Physics and Astronomy, University of Birmingham, Birmingham B15 2TT*

Received: Accepted:

ABSTRACT

We test the hypothesis that the apparent axis ratio of an elliptical galaxy is correlated with the age of its stellar population. We find that old ellipticals (with estimated ages $t > 7.5$ Gyr) are rounder on average than younger ellipticals. The statistical significance of this shape difference is greatest at small radii; a Kolmogorov–Smirnov test comparing the axis ratios of the two populations at $R = R_e/16$ yields a statistical significance greater than 99.96%. The relation between age and apparent shape is linked to the core/power-law surface brightness profile dichotomy. Core ellipticals have older stellar populations, on average, than power-law ellipticals and are rounder in their inner regions. Our findings are consistent with a scenario in which power-law ellipticals are formed in gas-rich mergers, while core ellipticals form in dissipationless mergers, with cores formed and maintained by the influence of a binary black hole.

Key words: Galaxies: elliptical – galaxies: evolution – galaxies: photometry – galaxies: structure

1 INTRODUCTION

In the standard classification scheme devised by Hubble (1926), the apparent shape of an elliptical galaxy is designated by a single number; each elliptical is given the label ‘En’, where n is ten times the ellipticity of the galaxy’s projected image, rounded to the nearest integer. In actuality, of course, the structure of an elliptical galaxy is too complicated to be summed up in a single number. When the surface brightness of an elliptical is fitted with elliptical isophotes of semimajor axis a and semiminor axis b , it is found that the axis ratio $q \equiv b/a$ is a function of the isophotal radius $R \equiv (ab)^{1/2}$. The majority of ellipticals have axis ratios q that decrease with R or remain roughly constant; however, some ellipticals become rounder with increasing R , or have $q(R)$ that varies irregularly (Bettoni et al. 1997).

It isn’t surprising that the shapes of elliptical galaxies can vary with radius, since the processes that sculpt galaxies are different in the inner and outer regions. It appears from a growing body of evidence that most, if not all, elliptical galaxies harbor a central supermassive black hole (Kormendy & Richstone 1995). A black hole can have a significant effect on the stellar distribution in an elliptical galaxy’s inner regions; by disrupting box orbits, it drives an initially triaxial galaxy to a more nearly axisymmetric shape (Ger-

hard & Binney 1985; Norman et al. 1985; Valluri & Merritt 1998). The outer regions of elliptical galaxies, particularly in rich clusters and compact groups, will be shaped by tidal encounters with neighboring galaxies.

At a given time, we expect the shape of an elliptical galaxy to be a function of radius. Moreover, at a given radius within a galaxy, we expect the shape to be a function of time. In the hierarchical clustering model for the formation of structure, ellipticals form by the merger of smaller galaxies. Mergers of galaxies with roughly equal mass create merger remnants which are flattened; the ratio of shortest to longest axis is typically $\gamma \equiv c/a \sim 0.5$ (Barnes 1992; Springel 2000). For a dissipationless merger, the elliptical remnant may be oblate, prolate, or triaxial, depending on the initial geometry of the merger (Barnes 1992). The presence of gas in the merging galaxies doesn’t strongly affect the axis ratio γ , but tends to make the remnant more nearly oblate (Springel 2000). Thus, the overall shape of an elliptical galaxy depends on whether the most recent major merger in its history was gas-rich or gas-poor. In addition, if each of the two merging progenitors contains a central black hole, the two black holes will significantly affect the structure of the merger remnant as they gradually spiral together and coalesce. By ejecting stars, the black hole binary carves out a central core with stellar density $\rho \propto r^{-\alpha}$, with $\alpha \sim 0.5$ (Ebisuzaki et al. 1991; Makino & Ebisuzaki 1996). The binary black hole undergoes a random walk as it ejects stars

* email: ryden@astronomy.ohio-state.edu

from the core (Merritt 2001), tending to create a cuspy core which is more nearly spherical than the flattened, $\gamma \sim 0.5$, merger remnant.

In view of these physical considerations, we expect the shape of an elliptical galaxy to depend on its merger history and to be modified in its central regions by the effects of massive black hole binaries. In general, elliptical galaxies formed in a major merger will become rounder with time (at least in their inner regions). The same physical processes that affect the shape of an elliptical galaxy may also modify its luminosity profile; thus, we might expect ‘core’ ellipticals to differ significantly in shape from ‘power-law’ ellipticals. The purpose of this paper is to test these naïve expectations by examining the projected axis ratios q of a sample of nearby bright elliptical galaxies, as a function of galaxy assembly age (t), isophotal radius (R), and luminosity profile type (core or power-law).

In section 2 of this paper, we describe how we assign an age t to each galaxy in our sample. In section 3, we describe how we determine the shape profile $q(R)$ for each galaxy. In section 4, we examine the relation between q and t at different fiducial radii. In section 5, we discuss how the age – shape relation differs for core ellipticals and for power-law ellipticals. Finally, in section 6, we consider how these results shed light on the evolution of elliptical galaxies and the origin of the core/power-law dichotomy.

2 AGE DETERMINATION

If an elliptical galaxy is formed by the successive merger of smaller galaxies, then assigning an age to that galaxy becomes an exercise in ambiguity. In this paper, we are concerned with how the shape of a galaxy changes as it evolves dynamically. Thus, the most useful definition of a galaxy’s age, for our purposes, is the time that has elapsed since the galaxy last underwent a major merger. If the merging galaxies contain gas, then the gas loses angular momentum during the course of the merger and flows to the centre, where it triggers a brief but intense burst of star formation (Barnes & Hernquist 1991, 1996; Mihos & Hernquist 1994, 1996). The time since the last major merger (if the merging progenitors contained significant amounts of gas) should be equal to the age of the youngest stars in the central region of the elliptical.

The age determinations used in this paper are drawn from the recent catalogue of Terlevich & Forbes (2000). This catalogue contains galaxies for which there exist high-quality H β and [MgFe] absorption line indices. Using the stellar population model of Worthey (1994), these line indices are used to break the age/metallicity degeneracy, giving separate age and metallicity estimates for the galaxies in the catalogue. The line indices used by Terlevich & Forbes (2000) come from the galaxies’ central regions and are luminosity weighted. Thus, they are dominated by the last major burst of star formation at the centre of each galaxy. The age determinations are therefore likely to reflect the time since the most recent major merger in the galaxy’s history. (One caveat must be added: if a major merger is purely dissipationless, it will not trigger a burst of star formation, and thus will not leave its mark on the stellar population.)

Terlevich & Forbes (2000) provide ages for ~ 150 rela-

tively nearby galaxies. We eliminated from our sample galaxies with estimated ages $t > 17$ Gyr; these galaxies may have authentically old stellar populations, but they may also be suffering from residual H β emission. Of the remaining galaxies, we select the 68 galaxies classified by Terlevich & Forbes as E galaxies, the 5 galaxies classified as cD galaxies (NGC 1399, NGC 2832, NGC 4839, NGC 4874, and IC 5358), and the one galaxy classified as cE (NGC 221); the morphological types used by Terlevich & Forbes were taken from the NASA/IPAC Extragalactic Database. The 74 galaxies in our sample are listed in Table 1, along with their ages as estimated by Terlevich & Forbes (2000). It is important to note that the overall calibration of the ages is somewhat uncertain, although the relative ranking of the ages is quite robust.

3 APPARENT SHAPE DETERMINATION

The 74 galaxies in our sample are relatively nearby, with distances ranging from 0.72 Mpc for NGC 221 to 112 Mpc for IC 5358, with a median distance of 23 Mpc (assuming $H_0 = 75 \text{ km s}^{-1} \text{ Mpc}^{-1}$). The galaxies are a mix of field galaxies and galaxies from groups and clusters, with 9 galaxies from the Fornax cluster, 11 from the Virgo cluster, and 11 from the Coma cluster. Most of the galaxies have photometric data available in the published literature. Values of the effective radius R_e for each galaxy in the sample were taken from Faber et al. (1989), when available. For those few galaxies not assigned a value of R_e by Faber et al. (1989), the effective radius was taken from other sources. Table 1 gives the adopted value of R_e for each galaxy.

Once a value of R_e was assigned to each galaxy, we used published isophotal data to find the axis ratio $q \equiv b/a$ at six reference radii: $R \equiv (ab)^{1/2} = 2^n R_e$, where $n = -4, -3, \dots, +1$. We found published isophotal fits based on ground-based data for 65 galaxies in our sample, and fits based on Hubble Space Telescope (HST) data for 29 galaxies in our data. We searched the HST archive for additional images in which galaxies from our sample were located on the PC chip of WFPC2. Galaxies with substantial central dust were excluded from analysis, leaving 24 additional galaxies. These were then modelled using the ISOPHOTE package in STSDAS. The sources of isophotal information for each galaxy are listed in Table 1. Fortunately, the axis ratio q is a robust parameter which does not significantly depend on the isophote-fitting algorithm used. Moreover, for elliptical galaxies, q does not strongly depend on the filter used. Thus, for galaxies with multiple sources of isophotal information, the values of q tabulated in Table 1 are simply the average value of q taken from all relevant sources. To minimize the effects of seeing, we discarded all isophotes with R less than 3 times the FWHM of the relevant observation (assumed to be 0.1 arcsec for HST).

4 THE AGE – SHAPE RELATION

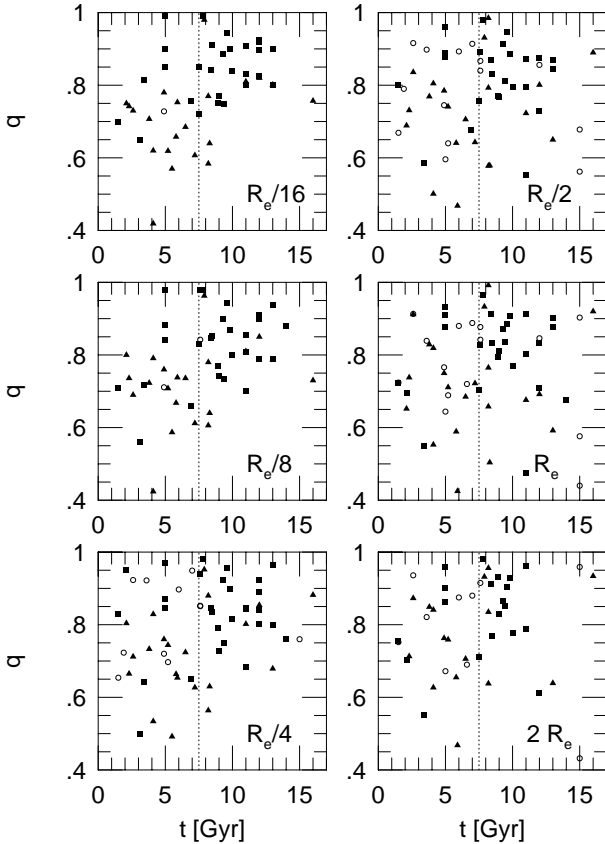
Figure 1 shows a plot of the apparent axis ratio q versus the computed galactic age t at our six reference radii, $R_e/16$ through $2R_e$. In each panel, each point represents a different galaxy. Particularly at the smallest reference radius, $R_e/16$,

Table 1. Elliptical galaxy ages and axis ratios

Galaxy name	Age [Gyr]	Profile type ^a	R_e [arcsec]	$q(R_e/16)$	$q(R_e/8)$	$q(R_e/4)$	$q(R_e/2)$	$q(R_e)$	$q(2R_e)$	Isophotal data	
										HST ^b	Ground-based ^c
NGC221	3.8	\	38.6	0.71	0.72	0.73	0.77	0.83	0.85	a	1
NGC315	4.9	-	58.5	0.73	0.71	0.72	0.74	0.77	-	b	2,3
NGC547	7.6	∩	12.6	-	0.98	0.94	0.89	0.83	-	z	4
NGC584	2.1	\	27.4	0.75	0.80	0.80	0.69	0.65	-	z	4
NGC636	3.6	-	18.9	-	-	0.92	0.90	0.84	0.82	-	4,5
NGC720	3.4	∩	39.6	0.81	0.72	0.64	0.58	0.55	0.55	c	3,4,6,7,8,9
NGC821	7.2	\	45.4	0.61	0.61	0.63	0.64	0.72	-	d	4,9
NGC1209	15.	-	17.7	-	-	-	0.56	0.44	0.43	-	7
NGC1339	7.5	∩	16.9	0.85	0.83	-	0.76	0.70	0.71	z	10
NGC1373	8.9	∩	11.8	0.75	0.77	0.79	0.77	0.79	0.93	z	10
NGC1374	9.8	∩	30.0	0.90	0.87	0.90	0.88	0.91	0.93	z	10
NGC1379	7.8	∩	42.4	0.99	0.98	0.98	0.98	0.96	0.98	z	5,10
NGC1399	5.0	∩	42.4	0.90	0.88	0.87	0.89	0.91	0.96	c	5,8,9,10
NGC1404	5.0	∩	26.7	0.85	0.84	0.85	0.88	0.88	0.86	z	5,9,10
NGC1419	8.2	\	10.9	0.77	0.78	0.88	0.98	0.99	0.96	z	10
NGC1427	6.5	\	32.9	0.68	0.74	0.72	0.71	0.68	0.71	e,f	9,10
NGC1453	7.6	-	28.0	-	-	0.85	0.84	0.84	-	-	4,8
NGC1549	7.6	-	47.6	-	0.84	0.85	0.87	0.88	0.92	-	5,9,11
NGC1600	6.9	∩	47.6	0.76	0.66	0.65	0.68	-	-	d,g	3,4
NGC1700	2.3	\	13.7	0.74	0.74	0.66	0.73	0.74	0.71	c,f	4,5,7,9
NGC2778	8.2	\	16.5	-	-	-	0.79	0.76	0.84	-	3
NGC2832	12.	∩	25.5	0.83	0.79	0.80	0.73	0.71	0.61	c	3,12
NGC2865	1.5	∩	11.7	0.70	0.71	0.83	0.80	0.72	0.75	z	11,13
NGC3078	14.	-	23.8	-	-	-	-	-	-	-	-
NGC3377	4.1	\	33.7	0.42	0.42	0.53	0.50	0.55	0.63	c	3,9,11
NGC3379	9.3	∩	35.2	0.89	0.90	0.92	0.91	0.87	0.87	g	3,4,9,11
NGC3585	3.1	∩	39.6	0.65	0.56	0.50	-	-	-	z	-
NGC3605	5.8	\	17.3	0.66	0.67	0.66	0.64	0.59	0.66	c	3,11
NGC3608	10.	∩	35.2	0.84	0.80	0.82	0.79	0.77	0.78	c,f	9,11
NGC3818	5.0	-	21.2	-	-	-	0.60	0.64	0.67	-	11
NGC4073	7.5	∩	55.9	0.72	-	-	-	-	-	z	-
NGC4239	5.5	\	16.1	0.57	0.59	0.49	-	-	-	c	-
NGC4261	9.4	∩	38.6	0.75	0.73	0.75	0.81	0.84	0.85	b,d	3,4,9,10
NGC4278	8.4	∩	32.9	0.84	0.85	0.85	0.87	0.91	0.91	f	3,9
NGC4339	7.9	\	30.7	0.98	0.96	0.95	0.93	0.93	0.93	z	10
NGC4374	11.	∩	54.6	0.83	0.81	0.85	0.87	0.91	0.96	b,d	3,4,9,11,14
NGC4387	13.	\	15.4	0.80	0.79	0.68	0.65	0.59	0.64	c	3,11,14
NGC4458	16.	\	26.7	0.76	0.73	0.88	0.89	0.92	0.93	c	11,14
NGC4472	8.5	∩	104.	0.91	0.85	0.83	0.83	0.83	0.77	g	3,4,10
NGC4478	4.1	\	14.0	0.62	0.79	0.83	0.80	0.82	0.84	h	3,11,14
NGC4489	2.6	-	32.2	-	-	0.92	0.92	0.91	0.94	-	11
NGC4551	5.2	\	17.7	0.62	0.71	0.74	0.74	0.71	0.76	c	3,11,14
NGC4552	9.6	∩	30.0	0.94	0.94	0.96	0.95	0.88	0.90	f,g	4,14
NGC4564	5.9	\	21.7	0.75	0.74	0.65	0.47	0.42	0.47	h	9,14
NGC4649	11.	∩	73.6	0.91	0.86	0.84	0.80	0.80	0.79	g	3,4,14
NGC4697	8.2	\	75.4	0.58	0.61	0.56	0.58	0.66	0.64	c	3,6,9,11
NGC4839	15.	-	28.6	-	-	0.76	0.68	0.58	-	-	13
NGC4860	12.	∩	8.6	0.92	0.90	0.84	-	-	-	z	-
NGC4869	15.	-	8.5	-	-	-	-	0.90	0.96	-	2,13
NGC4874	13.	∩	61.2	0.90	0.94	0.96	0.87	0.90	-	c	3,13
NGC4876	2.1	∩	6.0	-	-	0.95	-	0.70	0.70	z	13
NGC4908	12.	-	9.5	-	-	-	-	-	-	-	-
NGC4926	13.	∩	11.4	0.80	0.79	0.80	0.84	0.88	-	z	13
NGC4952	6.6	-	9.0	-	-	-	-	0.72	0.69	-	15
NGC4957	4.9	\	14.7	0.78	0.76	0.76	0.78	0.75	0.76	z	15
NGC5018	1.5	-	25.0	-	-	0.65	0.67	0.72	0.75	-	9
NGC5638	7.0	-	28.0	-	-	0.95	0.91	0.89	0.88	-	3,11
NGC5812	5.0	∩	23.8	0.99	0.98	0.97	0.96	0.93	0.90	z	8
NGC5831	2.6	\	26.7	0.73	0.69	0.71	0.84	0.91	0.87	z	3,11
NGC5846	12.	∩	82.6	0.92	0.91	0.92	-	-	-	z	4
NGC6127	9.3	-	21.7	-	-	-	-	-	-	-	-
NGC6702	1.9	-	28.6	-	-	0.72	0.79	-	-	-	4
NGC6958	12.	-	20.8	-	-	-	0.86	0.85	-	-	8

Table 1 – *continued*

Galaxy	Age [Gyr]	Profile type ^a	R_e [arcsec]	$q(R_e/16)$	$q(R_e/8)$	$q(R_e/4)$	$q(R_e/2)$	$q(R_e)$	$q(2R_e)$	Isophotal data	
										HST ^b	Ground-based ^c
NGC7052	11.	\cap	20.8	0.80	0.70	0.68	0.55	0.48	-	b,d	2,4
NGC7454	5.2	-	24.4	-	-	0.70	0.64	0.69	-	-	4
NGC7562	11.	\backslash	23.8	0.81	0.81	0.80	0.72	0.68	-	z	4,8
NGC7619	9.0	\cap	32.2	0.77	0.74	0.73	0.77	0.81	0.83	z	4,5
NGC7626	12.	\cap	37.8	0.90	0.90	0.89	0.87	0.83	-	b,d,e,f	2,3,4,5,8
NGC7785	8.3	\backslash	26.7	0.64	0.64	0.63	0.58	0.50	-	z	4,8
IC2006	6.0	-	28.6	-	-	0.90	0.89	0.88	0.88	-	16
IC4045	14.	\cap	5.7	-	0.88	0.76	-	0.68	-	z	13
IC4051	12.	\backslash	22.9	0.82	0.85	0.85	0.80	0.70	-	z	13
IC5358	16.	-	18.5	-	-	-	-	-	-	-	-
E274G06	12.	-	-	-	-	-	-	-	-	-	-

^a \backslash = Power-law, \cap = Core^b (a) Lauer et al. 1998, (b) Verdoes Kleijn et al. 1999, (c) Lauer et al. 1995, (d) Quillen et al. 2000, (e) Forbes et al. 1995, (f) Carollo et al. 1997, (g) Lauer et al. 2000, (h) van den Bosch et al. 1994, (z) this work.^c (1) Peletier 1993, (2) de Juan et al. 1994, (3) Peletier et al. 1990, (4) Lauer 1985, (5) Franx et al. 1989, (6) Jedrzejewski et al. 1987, (7) Capaccioli et al. 1988, (8) Sparks et al. 1991, (9) Goudfrooij et al. 1994, (10) Caon et al. 1994, (11) Jedrzejewski 1987, (12) Postman & Lauer 1995, (13) Jorgensen et al. 1992, (14) Caon et al. 1990, (15) Mehlert et al. 2000, (16) Schweizer et al. 1989.**Figure 1.** Isophotal axis ratio q as a function of age estimate t at $R = R_e/16, R_e/8, R_e/4, R_e/2, R_e$, and $2R_e$. Galaxies with core profiles are indicated by squares, galaxies with power-law profiles are indicated by triangles, and galaxies with unknown profile type are indicated by open circles.

there is a significant correlation between q and t , with old galaxies tending to be rounder than young galaxies. The tightness of the correlation decreases at larger radii.

To quantify the statistical significance of the difference in shape between young and old ellipticals, we ran a number

of Kolmogorov–Smirnov tests, comparing the distribution of q for young galaxies ($t \leq t_0$) with that for old galaxies ($t > t_0$). By computing the KS probability P_{KS} for different values of the dividing time t_0 , we found $t_{0,m}$, the value of t_0 which minimizes P_{KS} , and hence maximizes the shape difference between young and old ellipticals. Interestingly, for all six of our reference radii, P_{KS} is minimized at $t_{0,m} \approx 7.5$ Gyr. (At $R = R_e/16$, there is an additional minimum in P_{KS} , of comparable depth, at $t_0 = 9.5$ Gyr). Since the sample of galaxies used to determine $t_{0,m}$ is different at different values of R , though, the prudent reader should not place too much emphasis on the dependence of $t_{0,m}$; the more physically significant relation is the dependence of q on t at a given value of R . For the rest of this paper, we will define ‘young’ ellipticals as having $t \leq 7.5$ Gyr and ‘old’ ellipticals as having $t > 7.5$ Gyr. Table 2 gives the numbers N_{young} and N_{old} of young and old ellipticals in our sample at each reference radius, as well as the mean axis ratios \bar{q}_{young} and \bar{q}_{old} and the KS probability measuring the difference in the shape distribution for young and old galaxies. Although the probability $P_{KS} = 0.0034$ measured at $R_e/16$ is impressively small, remember that the dividing line $t_0 = 7.5$ Gyr between young and old galaxies was specifically chosen to minimize P_{KS} , and not set *a priori* from independent considerations. To test the true statistical significance of the difference in $q(R_e/16)$ between young and old galaxies, we did an analysis involving bootstrap resampling. There are 50 galaxies in our sample for which $q(R_e/16)$ was measured. Let $(t_1, t_2, \dots, t_{50})$ be the estimated ages of these galaxies and $(q_1, q_2, \dots, q_{50})$ be their values of $q(R_e/16)$. For each resampling of the data, we randomly drew 50 values of t , with replacement, from $(t_1, t_2, \dots, t_{50})$ and paired them with 50 values of q drawn randomly, with replacement, from $(q_1, q_2, \dots, q_{50})$. For these 50 random (t, q) pairs, we found the value of t_0 which minimizes the value of P_{KS} when comparing the values of q for galaxies with $t > t_0$ to those of galaxies with $t \leq t_0$. After performing 10^6 resamplings, we found that a fraction $f = 0.0012$ of the resampled data sets had a minimized P_{KS} less than 0.00034, the value found for the original data set. For comparison, when we did the same analysis using $q(R_e)$

Table 2. Difference in axis ratio for young ($t \leq 7.5$ Gyr) and old ($t > 7.5$ Gyr) ellipticals

R	N_{young}	\bar{q}_{young}	N_{old}	\bar{q}_{old}	P_{KS}
$R_e/16$	23	0.722	27	0.835	0.00034
$R_e/8$	22	0.721	30	0.830	0.0017
$R_e/4$	29	0.748	32	0.829	0.0066
$R_e/2$	28	0.747	32	0.804	0.077
R_e	28	0.744	34	0.789	0.087
$2R_e$	24	0.763	22	0.834	0.037

as the fiducial axis ratio, we found that a fraction $f = 0.43$ of the resampled data sets had a minimized P_{KS} less than 0.087, the value for the original data set. Thus, we may conclude that the difference in shape between young and old galaxies is not statistically significant at $R = R_e$, but is significant at $R = R_e/16$.

Terlevich & Forbes (2000) found only a weak correlation between apparent axis ratio and age for the elliptical galaxies in their catalogue; however, the axis ratios they used were measured at the effective radius, and at R_e , as we have seen, the difference in shape between young and old ellipticals is not statistically significant.

The statistical significance of the difference in shape between young and old galaxies at small radii ($R = R_e/16$) is not highly dependent on the choice of the dividing time t_0 between old and young galaxies; $P_{\text{KS}} < 0.01$ for all values of t_0 in the range $4.1 \text{ Gyr} < t_0 < 11 \text{ Gyr}$. A dividing time t_0 of several gigayears is very much longer than the dynamical time t_{dyn} at $R = R_e/16$; for the galaxies in our sample, the dynamical time at $R = R_e/16$ is of order $t_{\text{dyn}} \sim 1 \text{ Myr}$.

Given a sample q_1, q_2, \dots, q_N of apparent axis ratios, it is possible to use kernel density estimators to approximate the underlying distribution function $f(q)$ for the apparent axis ratios. The upper panel of Figure 2 shows the kernel estimate for the distribution of q measured at small radii ($R = R_e/16$) for young ellipticals ($t \leq 7.5 \text{ Gyr}$). A Gaussian kernel was used with a bandwidth $h = 0.056$. The bandwidth used was computed from the formula $h = 0.9\sigma N^{-0.2}$, where σ is the standard deviation of the sample; this value of h minimizes the integrated mean square error for samples which are not strongly skewed (Silverman 1986; Vio et al. 1994). The solid line is the best fit found to the data. The dashed lines give the 80 percent confidence interval, found by bootstrap resampling of the original data set. That is, at any value of q , 10 percent of the estimates found by bootstrap resampling lie above the upper dashed line and 10 percent lie below the lower dashed line. The dotted lines give the 98 percent confidence interval, found by the same bootstrap technique. The scarcity of nearly circular isophotes ($q \gtrsim 0.8$) is a characteristic signature of a population of triaxial objects. However, given the small sample size ($N = 23$) of young elliptical galaxies with isophotal data at $R = R_e/16$, the strongest statement we can make is that if the inner regions of young ellipticals are randomly oriented and spheroidal (either oblate or prolate), few of them can have an intrinsic axis ratio $\gamma \gtrsim 0.8$.

The lower panel of Figure 2 shows the kernel estimate for the distribution of q measured at small radii ($R = R_e/16$) for old ellipticals ($t > 7.5 \text{ Gyr}$). A Gaussian kernel was used with a bandwidth $h = 0.043$. As compared to the young ellipticals, the old ellipticals are more likely to have nearly

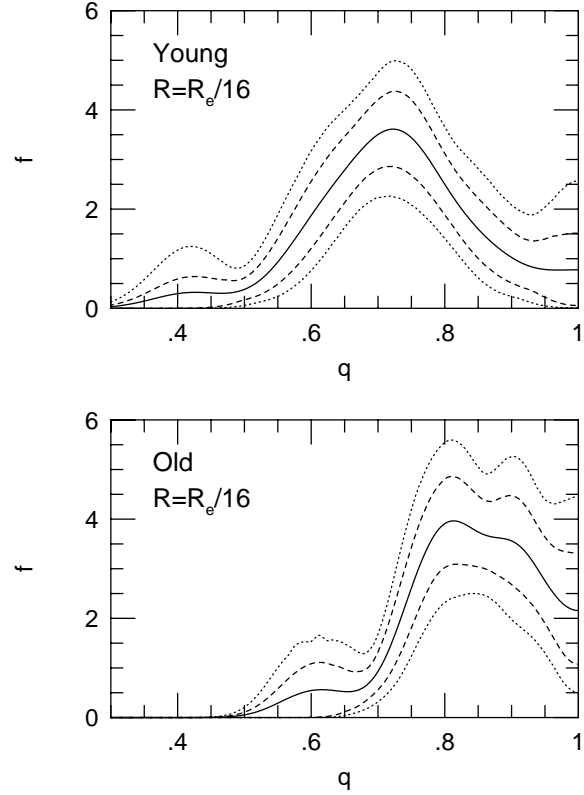


Figure 2. (Upper panel) The distribution function for the apparent axis ratio q of young ($t \leq 7.5 \text{ Gyr}$) elliptical galaxies, as measured at $R = R_e/16$. The solid line is the best fit, the dashed lines are the 80 percent confidence interval, and the dotted lines are the 98 percent confidence interval. (Bottom panel) The same, but for the old ($t > 7.5 \text{ Gyr}$) elliptical galaxies in the sample.

circular central isophotes ($q \gtrsim 0.8$). The observed apparent shapes are consistent with the hypothesis that the central regions of old ellipticals are oblate; they are also consistent with the hypothesis that they are prolate. In sum, the apparent shapes of young and old ellipticals are consistent with a scenario in which the central regions of elliptical galaxies evolve from being flattened triaxial ellipsoids to being nearly spherical oblate spheroids; however, the data do not require such a scenario.

5 CORE VERSUS POWER-LAW

The intrinsic axis ratios of an elliptical galaxy may change with time; so may its luminosity profile. Elliptical galaxies can be divided into two classes, based on the shape of their luminosity profiles. Power-law ellipticals have luminosity densities in their inner regions which are well fitted by a pure power law all the way to the limit of resolution. Core ellipticals, by contrast, have luminosity densities which show a break to a shallower inner slope (Ferrarese et al. 1994; Forbes et al. 1995; Lauer et al. 1995). The break radius for core galaxies is generally a few percent of the effective radius (Faber et al. 1997); thus, for a typical core elliptical,

our innermost reference radius at $R = R_e/16$ is comparable to, or slightly larger than, the break radius.

The discovery of the core/power-law dichotomy has led to speculation about its cause. In the scenario of Faber et al. (1997), power-law ellipticals form in gas-rich mergers. In such a merger, dissipation and angular momentum transfer permits the gas to fall toward the centre, and naturally give rise to a steep power-law profile in the merger remnant (Barnes & Hernquist 1991, 1996; Mihos & Hernquist 1994, 1996). We might expect the gaseous nature of the power-law galaxies' formation to be accompanied by a burst of star formation and the formation of a stellar disc (de Jong & Davies 1997). The origin of core ellipticals is more problematic. Faber et al. (1997) suggest that core galaxies form in largely dissipationless mergers; a low-density core is 'scoured out' by the black hole binary which forms by orbital decay of the black holes in the progenitor galaxies (Eisuzaki et al. 1991; Makino & Eisuzaki 1996). The central black hole which results from the coalescence of the binary maintains the central low density of the core by tidally disrupting any high-density satellite galaxies subsequently accreted by the core elliptical (Faber et al. 1997; Merritt & Cruz 2001).

To test the correlation among age, profile type, and isophote axis ratio, we have determined the profile type (core or power-law) for as many of the 74 ellipticals in our galaxy sample as possible (either from the literature or deriving them ourselves). The resulting profile types are given in Table 1. In assigning profile types, we followed the definition of Faber et al. (1997) that a core galaxy has a surface density profile with a logarithmic slope $d \log I / d \log R > -0.3$ inside its break radius. In the case of NGC 7626, HST WFPC2 imaging yields a core profile at V and I (Carollo et al. 1997), but NICMOS imaging yields a power-law profile at $1.6\mu\text{m}$ (Quillen et al. 2000). We assign NGC 7626 a core profile, for consistency with other systems for which only V or I images are available.

Of the 74 ellipticals in our sample, 53 had HST images which permitted classification of their profile type. The 22 power-law galaxies have a mean and standard deviation for their ages of $t = 6.9 \pm 3.5$ Gyr. For the 29 core galaxies, the mean and standard deviation are $t = 8.6 \pm 3.3$ Gyr. Figure 3 shows the distribution function for the ages of the power-law galaxies (top panel) and the core galaxies (bottom panel). A KS test comparing the distribution of ages for the two different types of galaxy yields $P_{\text{KS}} = 0.017$.

The power-law galaxies are significantly younger, on average, than the core galaxies. Of the power-law galaxies, 13 fall into the 'young' category ($t \leq 7.5$ Gyr) and 9 into the 'old' category. Of the core galaxies, by contrast, only 8 are young and 23 are old. Since profile type correlates with age, and age correlates with axis ratio (in the central regions of a galaxy), it is not surprising that profile type correlates with axis ratio. In Figure 1, the core galaxies (symbolised by squares) and the power-law galaxies (symbolised by triangles) lie in different regions of the $q-t$ plane. Particularly when q is measured at $R = R_e/16$, it is seen that power-law galaxies are younger and flatter; core galaxies are older and rounder. Table 3 gives the numbers N_{power} and N_{core} of power-law and core ellipticals in our sample at each reference radius, as well as the mean axis ratios \bar{q}_{power} and \bar{q}_{core} and the KS probability measuring the difference in the shape distribution for power-law and core ellipticals. Note

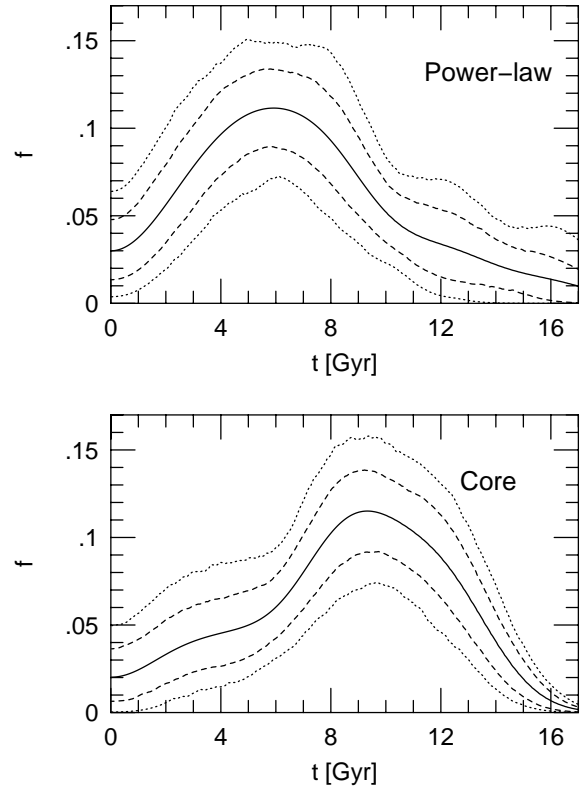


Figure 3. (Upper panel) The distribution function for the ages of power-law galaxies, as found by a kernel density estimator. The solid line is the best fit, the dashed lines are the 80 percent confidence interval, and the dotted lines are the 98 percent confidence interval. (Bottom panel) The same information for the core galaxies in the sample.

Table 3. Difference in axis ratio for power-law and core ellipticals

R	N_{power}	\bar{q}_{power}	N_{core}	\bar{q}_{core}	P_{KS}
$R_e/16$	21	0.705	28	0.843	0.00041
$R_e/8$	21	0.721	29	0.830	0.0033
$R_e/4$	21	0.723	29	0.830	0.012
$R_e/2$	21	0.726	25	0.822	0.027
R_e	21	0.720	26	0.808	0.020
$2R_e$	16	0.762	20	0.828	0.35

that at most radii, the difference in shape between power-law and core ellipticals is comparable in significance to the difference in shape between young and old ellipticals. This difference in shape between core and power-law ellipticals was indirectly uncovered by Tremblay & Merritt (1996), who found that ellipticals brighter than $M_B = -20$ were rounder in projection than fainter ellipticals. Since ellipticals brighter than $M_B = -20$ are predominantly core galaxies while those fainter are predominantly power-law galaxies, the dependence of shape on luminosity is a reflection of the dependence of shape upon profile type.

The upper panel of Figure 4 shows the kernel estimate for the distribution of q at small radii ($R = R_e/16$) for the power-law ellipticals in our sample. A Gaussian kernel was used with a bandwidth $h = 0.056$. Note, in the

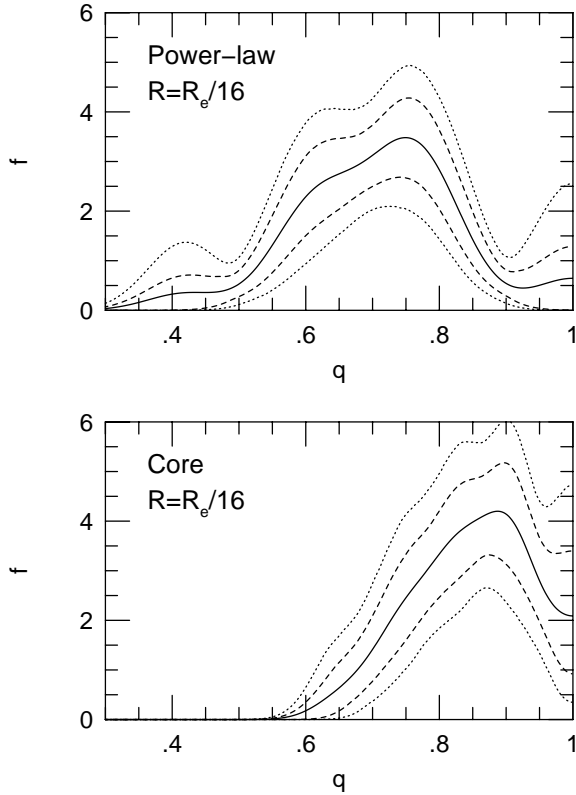


Figure 4. (Upper panel) The distribution function for the apparent axis ratio q of power-law ellipticals, as measured at $R = R_e/16$. The solid line is the best fit, the dashed lines are the 80 percent confidence level, and the dotted lines are the 98 percent confidence level. (Bottom panel) The same, but for the core ellipticals in the sample.

best-fitting estimate (given by the solid line), the scarcity of power-law galaxies with nearly circular isophotes. Of the 21 power-law ellipticals with isophotal information at $R_e/16$, only one (NGC 4339) has $q > 0.82$. This scarcity of round isophotes is highly implausible in a population of randomly oriented oblate spheroids. For such a population, the distribution function of the intrinsic axis ratio γ that minimizes the number of nearly circular isophotes is a delta function at $\gamma = 0$ (reflecting a population of infinitesimally thin discs). This distribution for γ produces a uniform distribution for q over the range $0 \leq q \leq 1$. Thus, for a population of infinitesimally thin circular discs, which *minimizes* the number of nearly circular isophotes given the oblate hypothesis, the probability of seeing 0 or 1 galaxies out of 21 with $q > 0.82$ is only $P = (0.82)^{21} + 21(0.82)^{20}(0.18) = 0.086$. For a more plausible distribution of γ (that is, one that would not overestimate the number of galaxies with small q), the probability P of finding so few nearly circular isophotes would be smaller still.

The distribution of q for core ellipticals, as measured at $R = R_e/16$, is displayed in the lower panel of Figure 4. A Gaussian kernel was used, with $h = 0.039$. For the sample of core galaxies, there is no scarcity of nearly circular isophotes. Of the 28 core ellipticals with isophotal information at $R_e/16$, 18 have $q > 0.82$. Neither the oblate or prolate

hypothesis can be rejected. If the inner regions of core ellipticals are oblate, the mean intrinsic axis ratio is $\bar{\gamma}_o = 0.75$; if the inner regions are prolate, the mean intrinsic axis ratio is $\bar{\gamma}_p = 0.78$.

In summary, the distribution of axis ratios for power-law ellipticals, as measured at $R = R_e/16$, is inconsistent with the hypothesis that their central regions are randomly oriented oblate spheroids. The distribution of axis ratios for core ellipticals, at the same reference radius, is consistent with the hypothesis that they are randomly oriented and spheroidal (either oblate or prolate).

6 IMPLICATIONS

We have shown that elliptical galaxies with estimated assembly ages $t > 7.5$ Gyr are rounder in projection than younger ellipticals; the statistical significance of the shape difference is greater at smaller radii. Similarly, we have shown that core elliptical galaxies are rounder in projection than power-law ellipticals; the significance of the shape difference is likewise greater at smaller radii. It is no coincidence that the solid lines in the two panels of Figure 3, giving the age distribution for power-law and core galaxies, intersect at an age $t \approx 7.5$ Gyr. Our sample of old galaxies, with $t > 7.5$ Gyr, consists primarily of core ellipticals, while our sample of young galaxies, with $t \leq 7.5$ Gyr, consists mainly of power-law galaxies.

Our results are consistent with the Faber et al. (1997) scenario, in which power-law galaxies form in gas-rich mergers and core ellipticals form in dissipationless mergers, with shallow density cores created and maintained by the influence of central black holes. The core elliptical galaxies have relatively old stellar ages, in this scenario, since their most recent major merger was dissipationless, without an accompanying burst of star formation. Since the core scoured out by a central black hole tends to be nearly spherical (Merritt 2000), it would also explain why the central isophotes of core ellipticals tend to be nearly spherical. By contrast, the gas-rich mergers which form power-law galaxies are accompanied by a burst of star formation, and tend result in the formation of a central stellar disc (de Jong & Davies 1997). Thus, the age t of a power-law galaxy reflects the time since the merger in which it was created; the flattened central isophotes of power-law galaxies reflect the presence of the disc which formed in the merger.

One question that arises, though, is why there are so few old power-law galaxies. There was no shortage of gas-rich mergers at $t > 7.5$ Gyr; indeed, the ratio of gas-rich to gas-poor mergers tends to decrease with time. One way in which old power-law galaxies are destroyed is through mergers. If a power-law galaxy undergoes a dissipational merger, the resulting galaxy will still have a power-law profile, but will have a younger age t , thanks to the star formation which accompanies a dissipational merger. If, by contrast, a power-law galaxy undergoes a dissipationless merger with a large core elliptical, the resulting galaxy will have a core profile, as the central density cusp of the power-law galaxy is disrupted by the central black hole of the core elliptical (Merritt & Cruz 2001). Thus, mergers tend to convert old power-law galaxies (where ‘old’ is a description of the age of the central stellar population) into young power-law galaxies if the

merger is gas-rich, or into old core galaxies if the merger is gas-poor.

At all events, the observed correlation among luminosity profile type, axis ratio, and age of stellar population provides a useful constraint for all future studies of the origin of the core/power-law dichotomy.

ACKNOWLEDGMENTS

We would like to thank M. Merrifield for acting as match-maker. I. Jorgensen and A. Quillen kindly provided data in electronic form. D. Merritt, T. Lauer, D. Richstone, and the anonymous referee made useful comments. This research has made use of the NASA/IPAC Extragalactic Database (NED) which is operated by the Jet Propulsion Laboratory, California Institute of Technology, under contract with the National Aeronautics and Space Administration.

REFERENCES

- Barnes, J. 1992, *ApJ*, 393, 484
 Barnes, J. E., & Hernquist, L. 1991, *ApJ*, 370, L65
 Barnes, J. E., & Hernquist, L. 1996, *ApJ*, 471, 115
 Bettoni, D., Fasano, G., Kjaergaard, P., & Moles, M. 1997, in Arnaboldi, M., Da Costa, G. S., & Saha, P. eds, *The Second Stromlo Symposium: The Nature of Elliptical Galaxies*. ASP, San Francisco, p. 71
 Caon, N., Capaccioli, M., & Rampazzo, R. 1990, *A&AS*, 86, 429
 Caon, N., Capaccioli, M., & D’Onofrio, M. 1994, *A&AS*, 106, 199
 Capaccioli, M., Pionto, G., & Rampazzo, R. 1988, *AJ*, 96, 487
 Carollo, C. M., Franx, M., Illingworth, G. D., & Forbes, D. A. 1997, *ApJ*, 481, 710
 de Jong, R. S., & Davies, R. L. 1997, *MNRAS*, 285, L1
 de Juan, L., Colina, L., Perez-Fournon, I. 1994, *ApJS*, 91, 507
 Ebisuzaki, T., Makino, J., & Okumura, S. K. 1991, *Nature*, 354, 212
 Faber, S. M., Wegner, G., Burstein, D., Davies, R. L., Dressler, A., Lynden-Bell, D., & Terlevich, R. J. 1989, *ApJS*, 69, 763
 Faber, S. M., et al. 1997, *AJ*, 114, 1771
 Ferrarese, L., van den Bosch, F. C., Ford, H. C., Jaffe, W., O’Connell, R. W. 1994, *AJ*, 108, 1598
 Forbes, D. A., Franx, M., & Illingworth, G. D. 1995, *AJ*, 109, 1988
 Franx, M., Illingworth, G., & Heckman, T. 1989, *AJ*, 98, 538
 Gerhard, O. E., & Binney, J. 1985, *MNRAS*, 216, 467
 Goudfrooij, P., Hansen, L., Jorgensen, H. E., Norgaard-Nielsen, H. U., de Jong, T., & van den Hoek, L. B. 1994, *A&AS*, 104, 179
 Hubble, E. 1926, *ApJ*, 64, 321
 Jedrzejewski, R. 1987, *MNRAS*, 226, 747
 Jedrzejewski, R. I., Davies, R. L., & Illingworth, G. D. 1987, *AJ*, 94, 1508
 Jorgensen, I., Franx, M., & Kjaergaard, P. 1992, *A&AS*, 95, 489
 Kormendy, J., & Richstone, D. 1995, *ARA&A*, 33, 581
 Lauer, T. R. 1985, *ApJS*, 57, 473
 Lauer, T. R. et al. 1995, *AJ*, 110, 2622
 Lauer, T. R., Faber, S. M., Ajhar, E. A., Grillmair, C. J., & Scowen, P. A. 1998, *AJ*, 116, 2263
 Lauer, T. R., et al. 2000, in preparation
 Magorrian, J., et al. 1998, *AJ*, 115, 2285
 Makino, J., & Ebisuzaki, T. 1996, *ApJ*, 465, 527
 Mehlert, D., Saglia, R. P., Bender, R., & Wegner, G. 2000, *A&AS*, 141, 449
 Merritt, D. 2000, preprint (astro-ph/9910546)
 Merritt, D. 2001, *ApJ*, submitted (astro-ph/00012264)
 Merritt, D., & Cruz, F. 2001, *ApJ*, submitted (astro-ph/0101194)
 Merritt, D., & Quinlan, G. 1998, *ApJ*, 498, 625
 Mihos, J. C., & Hernquist, L. 1994, *ApJ*, 431, L9
 Mihos, J. C., & Hernquist, L. 1996, *ApJ*, 464, 641
 Norman, C. A., May, A., & van Albada, T. S. 1985, *ApJ*, 296, 20
 Peletier, R. F. 1993, *A&A*, 271, 51
 Peletier, R. F., Davies, R. L., Illingworth, G. D., Davis, L. E., & Cawson, M. 1990, *AJ*, 100, 1091
 Postman, M., & Lauer, T. R. 1995, *ApJ*, 440, 28
 Quillen, A., Bower, G. A., & Stritzinger, M. 2000, *ApJS*, submitted (astro-ph/9907021)
 Quinlan, G. D., & Hernquist, L. 1997, *NewA*, 2, 533
 Ryden, B. S. 1996, *ApJ*, 461, 146
 Schweizer, F., van Gorkom, J. H., & Seitzer, P. 1989, *ApJ*, 338, 770
 Silverman, B. W. 1986, *Density Estimation for Statistics and Data Analysis* (New York: Chapman & Hall)
 Sparks, W. B., Wall, J. V., Jorden, P. R., Thorne, D. J., & van Breda, I. 1991, *ApJS*, 76, 471
 Springel, V. 2000, *MNRAS*, 312, 859
 Terlevich, A. I., & Forbes, D. A., 2000, *MNRAS*, submitted
 Tremblay, B., & Merritt, D. 1996, *AJ*, 111, 2243
 Valluri, M., & Merritt, D. 1998, *ApJ*, 506, 686
 van den Bosch, F. C., Ferrarese, L., Jaffe, W., Ford, H. C., & O’Connell, R. W., 1994, *AJ*, 108, 1579
 Verdoes Kleijn, G. A., Baum, S., de Zeeuw, P. T., & O’Dea, C. P. 1999, *AJ*, 118, 2592
 Vio, R., Fasano, G., Lazzarin, M., & Lessi, O. 1994, *A&A*, 289, 640